The relaxation factors chosen (both equal to 0.5) dramatically improve the convergence of the two cases for which $\bar{q}_{\text{div}} < 0$. Although these factors worsen the convergence of the first case ($\bar{q}_{\text{div}} > \bar{q} > 0$), the iterations still converge.

Conclusions

The problem of convergence of iterative static aeroelastic solutions are discussed using a linear simulation. The intimate relationship of the flight and divergence dynamic pressures to the convergence behavior is derived and illustrated. Rigorous criteria are derived for selecting the relaxation factors to ensure convergence of the iterations for a linear system. Knowledge of the divergence speed for a linearized point in a nonlinear iteration should be of benefit to convergence of the nonlinear iteration.

References

[1]Rodden, W. P., and Love, J. R., "Equations of Motion of a Quasisteady Flight Vehicle Utilizing Restrained Static Aeroelastic Characteristics," *Journal of Aircraft*, Vol. 22, No. 9, 1985, pp. 802–809.

[2]Jolley, L. B. W., *Summation of Series*, Dover, New York, 1961, Series A, p. 2.

[3]Sensburg, O., Schweiger, J., Gödel, H., and Lotze, A., "Integration of Structural Optimization in the General Design Process for Aircraft," *Journal of Aircraft*, Vol. 31, No. 1, 1994, pp. 206–212.

[4]Bisplinghoff, R., Ashley, H., and Halfman, R., *Aeroelasticity*, Addison–Wesley, Reading, MA, 1955, Chap. 8.

Effect of a Splitter Plate on Transonic Wing Flow: A Numerical Study

G. Lombardi* and M. V. Salvetti†
University of Pisa, Pisa 56126, Italy

Introduction

In the experimental analysis of the flow around isolated wings, semimodels mounted on a sidewall are widely used. Indeed, this approach is very attractive, because supports are not needed, and, hence, the effects of the interference between models and supports are eliminated. On the other hand, the flow at the root of the semimodel is clearly different from that at the symmetry plane of the isolated wing, due to the effect of the sidewall boundary layer, as pointed out in Ref. 1 for a low-aspect-ratio wing. To reduce this effect, the model is commonly offset from the tunnel sidewall by means of a splitter plate. Nevertheless, even in this case, the splitter-plate boundary layer may significantly affect the experimental data. Furthermore, on a forward-swept wing in transonic flow, a strong shock wave is present in the wing root region; hence, significant interactions may occur between this shock wave and the sidewall boundary layer.

The motivation of the present study arises from the discrepancies observed at the wing root between experimental data and the results of a Navier–Stokes solver for the transonic flow around a forward-swept wing of high-aspect ratio.[2] Because these discrepancies are limited to the wing root region and good agreement is found on the remainder of the wing, a possible explanation is the influence of the sidewall boundary layer on the experimental data. Therefore, in the present paper, the effects of a sidewall boundary layer on the transonic flow around a forward-swept wing are numerically investigated.

Experimental Conditions and Numerical Method

The tests, carried out in the Medium Speed Wind Tunnel of the Council for Scientific and Industrial Research facilities, in South Africa, are described in Refs. 3 and 4. The wing model has zero twist and dihedral angles, a negative sweep angle ($\Lambda = -25$ deg, at one-quarter of the chord); aspect ratio $= 5.7$; taper ratio $= 0.4$; and NACA 0012 wing sections. The splitter plate used in the experiments is described in Ref. 4. Pressure measurements are available at 10 span stations and 32 chord points.[3] The measurement procedure and accuracy are described in Ref. 4. The data obtained in transonic regime ($M = 0.7$), at $Re \approx 2.8 \times 10^6$, based on the mean aerodynamic chord, are considered in this Note.

For the numerical solution of the Navier–Stokes equations, the commercial code RAMPANT[5] (developed by FLUENT) is used. Three-dimensional compressible Navier–Stokes or Reynolds-averaged Navier–Stokes equations can be solved. The numerical method is based on a finite volume formulation and is second-order accurate in space. Steady solutions are obtained by time-marching the equations with an explicit, multistage, Runge–Kutta scheme with multigrid convergence acceleration. The solution is considered to have reached convergence after a three-order-of-magnitude reduction of the rms residual for each of the conserved variables. A more detailed description of the numerical procedure can be found in Ref. 2.

In all of the simulations, the external boundary is represented by a cylinder of circular section, with a radius of 6.75 mean aerodynamic chords and a spanwise length of 2.5 wingspans, starting from the wing root. An analysis of the sensitivity to the dimensions of the computational domain was carried out, indicating that, for the domain used here, the influence of the external boundary conditions on the solution is negligible. All of the results presented next are obtained by solving the Reynolds-averaged Navier–Stokes equations with the standard k-ε model.

Analysis of the Results

In Fig. 1, the chordwise pressure distributions obtained in the numerical simulation, for the isolated wing at an angle of attack of 8 deg, are compared with the experimental data at two spanwise sections. The computational grid has approximately 175×10^3 cells. Figure 1b shows that at 40% of the semispan [$y/(b/2) = 0.4$], the numerical results are in good agreement with the experimental data. Conversely, at $y/(b/2) = 0.04$ (Fig. 1a), the position and intensity of the shock wave obtained numerically are completely different from those observed experimentally. Moreover, in the experiments, the shock wave induces a separation of the boundary layer; whereas in the numerical simulation, the boundary layer remains attached. Another simulation on a grid of approximately 300×10^3 cells, locally refined in the wing root region, showed the grid independence of the results.[2] As discussed previously, a possible explanation of the discrepancy between experimental data and numerical results is the presence in the experiments of a splitter plate that could affect the measurements, particularly in the region close to the wing root. To investigate this effect, a numerical simulation of the flow around the wing mounted on the splitter plate has also been carried out. The computational grid used in this simulation has approximately the same resolution as that used for the isolated wing (the total number of cells is $\cong 500 \times 10^3$).

The numerical chordwise pressure distributions, obtained at $y/(b/2) = 0.04$ and $y/(b/2) = 0.4$ in this simulation, are compared with those over the isolated wing and with the experimental data, in Figs. 2a and 2b, respectively.

Figure 2 shows that the splitter plate strongly affects the position and intensity of the shock wave near the wing root. In the simulation with the splitter plate, the shock wave moves upstream by about 10% of the local chord with respect to the isolated wing case, and the agreement with the experimental data is noticeably improved. Moreover, the boundary layer separates immediately behind the shock wave, as in the experiments. Nevertheless, the pressure

Received 17 February 1997; revision received 19 October 1998; accepted for publication 26 January 1999.

*Assistant Professor, Department of Aerospace Engineering. Member AIAA.

†Assistant Professor, Department of Aerospace Engineering.

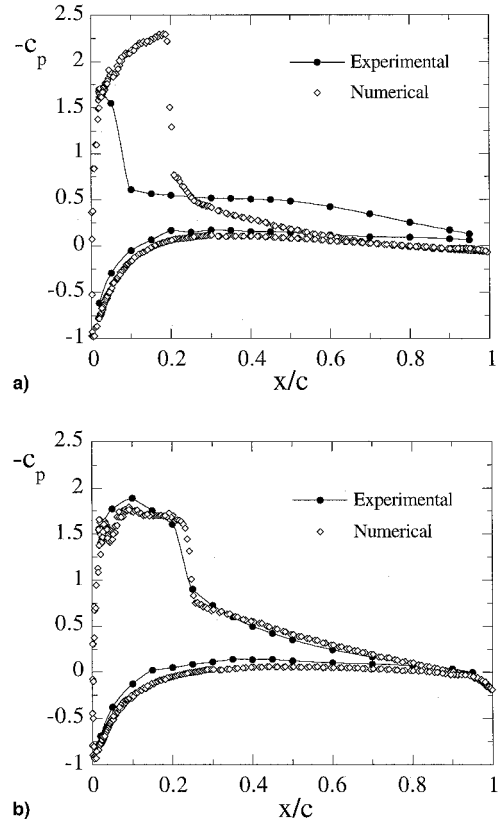

Fig. 1 Comparison between the chordwise pressure distribution obtained numerically for the isolated wing and the experimental data; $y/(b/2)$ = a) 0.04 and b) 0.40.

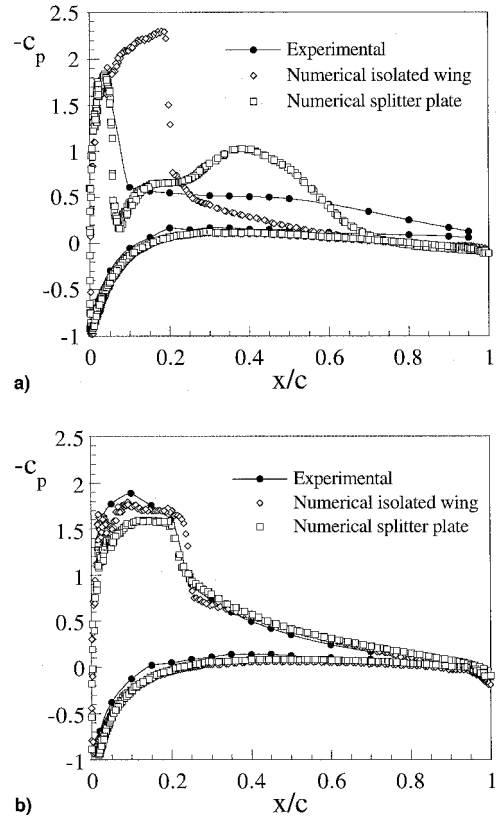

Fig. 2 Effect of the splitter plate on the chordwise pressure distributions; $y/(b/2)$ = a) 0.04 and b) 0.40.

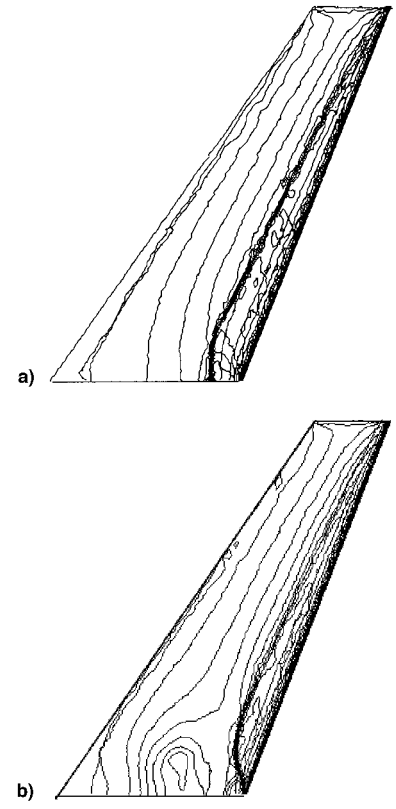

Fig. 3 Numerical pressure isocontours on the upper surface of the wing; c_p step = 0.2: a) isolated wing and b) wing mounted on the splitter plate.

distribution after the shock wave is different from the experimental one. A detailed analysis of the reasons for this discrepancy is beyond the scope of the present investigation and reference is made to Ref. 2. The aim of this study is to investigate whether the splitter plate affects the flow over the wing and if this effect may explain the discrepancy between experimental and numerical results, in particular, concerning the shock wave position.

Conversely, the pressure distribution in the remainder of the wing is not significantly affected by the splitter plate, as shown, e.g., in Fig. 2b. This result seems to be in contrast with the conclusions of a similar analysis carried out for a low-aspect-ratio wing in Ref. 1, in which the sidewall boundary layer was found to have a strong influence on the flowfield around the whole wing. Nevertheless, as pointed out in Ref. 1, the main effect of the sidewall boundary layer was to decrease the favorable spanwise pressure gradient, and, hence, to reduce the spanwise migration of the wing boundary layer. For the forward-swept wing considered in the present analysis, a strong crossflow is present in the inboard direction, and, hence, the sidewall boundary layer tends to remain confined close to the sidewall. This can be observed also from the pressure iso-contours in Fig. 3; the differences between the simulations with and without the splitter plate are localized in a very limited zone, close to the wing root (about 15% of the span). The recirculation bubble induced by the interaction with the splitter plate is also clearly visible in the wing root region.

Conclusions

The effects of a sidewall boundary layer on the transonic flow around a forward-swept wing have been numerically investigated. In particular, the flow over a configuration approximating the case of a semimodel mounted on a splitter plate has been simulated. The numerical results in the wing root region are strongly affected by the presence of the splitter plate, and noticeable better agreement with the experimental data is obtained in the simulation with the splitter plate than in that of the isolated wing, particularly as it concerns the shock-wave position. Nevertheless, the effects of the splitter

plate are confined to a very narrow zone near the wing root. This is probably due to the presence of a strong crossflow in the inboard direction, typical of forward-swept wings, that limits the spanwise propagation of the interference effects. Therefore, one may conclude that, for these types of wings, the experimental data are affected by the interference with the splitter plate only in a limited zone close to the wing root.

Acknowledgments

The present work has been financially supported by the Ministero della Università e Ricerca Scientifica. The authors gratefully acknowledge the Council for Scientific and Industrial Research of Pretoria, South Africa, for providing the experimental results.

References

[1]Milholen, W. E., II, and Chokani, N., "Effect of Sidewall Boundary Layer on Transonic Flow over a Wing," *Journal of Aircraft*, Vol. 31, No. 4, 1994, pp. 986–988.

[2]Lombardi, G., Salvetti, M. V., and Morelli, M., "Appraisal of Numerical Methods in Predicting the Aerodynamics of Forward-Swept Wing," *Journal of Aircraft*, Vol. 35, No. 4, 1998, pp. 561–568.

[3]Lombardi, G., "Experimental Aerodynamic Effects of a Forward Sweep Angle," *Journal of Aircraft*, Vol. 30, No. 5, 1993, pp. 629–635.

[4]Buresti, G., Lombardi, G., and Morelli, M., "Pressure Measurements on Different Canard-Wing Configurations in Subsonic Compressible Flow," Atti Del Dipartimento Di Ing. Aerospaziale Di Pisa, Rept. ADIA 91-4, Pisa, Italy, Sept. 1991.

[5]*RAMPANT User's Guide*, Release 4.0, Fluent, Lebanon, NH, April 1996.

Spreadsheet Fluid Dynamics

Etsuo Morishita*
University of Tokyo,
Hongo, Bunkyo-ku, Tokyo 113-8656, Japan

Nomenclature

Gr = Grashof number
Nu = Nusselt number
P = excess pressure
Pr = Prandtl number
p = static pressure
Ra = Rayleigh number ($=PrGr$)
Re = Reynolds number
T = temperature
t = time
u, v = velocity components
x, y = coordinates
ζ = vorticity
ψ = stream function

Introduction

COMPUTATIONAL fluid dynamics (CFD) is one of the most important branches of fluid dynamics. CFD enables a detailed analysis of flowfields, which otherwise is very difficult. In the learning stage of CFD, however, many researchers have had problems in regard to code development for scientific and engineering calculations, not only because of the complexity of the governing equations but also because of computer programming rules. This still often is the case among younger students who are just beginning to study numerical simulations.

Received 5 January 1998; revision received 10 February 1999; accepted for publication 22 February 1999.

*Professor, Department of Aeronautics and Astronautics, Graduate School of Engineering. Senior Member AIAA.

Currently available personal computer software, however, might enable us to do scientific computing without developing lengthy computer programs, depending on the situation. In particular, spreadsheet software is widely used at home and also for scientific calculations.[1] We realize that spreadsheets are extremely valuable for fluid dynamics simulations, as well as for other simulations.[2] The cells in the spreadsheet can be viewed as natural grids for computation and their assigned function can be iterated upon. Spreadsheets usually include graphics software and therefore the computational results can be visualized easily. When the spreadsheet is used for fluid dynamics calculations, we need the differential form of the governing equations and the boundary conditions. First, we define the computational domain in a spreadsheet. Typically, a steady two-dimensional fluid dynamics problem is assumed, e.g., a rectangular computational domain is selected. The boundary condition then is written in a cell on the boundary. This can be copied to other cells by copy-and-paste procedures. Before we write the boundary conditions, boundary cells should be colored, thereby making it easy to recognize the computational domain. Then, we write the governing equations in one of the cells in the computational domain. We copy the cell contents to other cells into the computational domain again by using spreadsheet copy-and-paste commands. Next we select the circular reference[1] calculation and decide on the number of iterations and the solution error tolerance. The computation is repeated automatically and we may continue the calculation until the desired convergence is achieved. When convergence is reached, we select the computational domain and visualize the results almost instantly using the inherent graphics software.

Spreadsheet fluid dynamics (SFD) is easy to use and does not require any special knowledge about the computer language being used (it is fair to say that it is already programmed). It is also possible to visualize the results during the computation and to interactively change the computational conditions, including the form of the equations and the boundary conditions.

SFD Procedure

We use Laplace's equation to illustrate the SFD procedure. The governing equation for the stream function of a potential flow is given by

$$\nabla^2 \psi = 0 \tag{1}$$

From the finite difference form of Eq. (1) for square grids, we can obtain at (x_i, y_j):

$$\psi_{i,j} = \frac{\psi_{i+1,j} + \psi_{i-1,j} + \psi_{i,j+1} + \psi_{i,j-1}}{4} \tag{2}$$

We used Eq. (2) for the potential flow over a step, shown in Fig. 1, i.e., a spreadsheet. The cells on the boundary should be colored for clarity. We specify the boundary conditions on the boundary cells. We input the value of the stream function on the boundary. So, in Fig. 1, $\psi = 0$ is used for the cells on the lower boundary (including the step), and $\psi = 1$ is used for the cells on the upper horizontal boundary. The inlet and outlet flows may be assumed to be uniform and a linear distribution of the stream function is used, i.e., $\psi = y$.

	A	B	C	D	E	F	G	H	I	J	K	L	M
1	dx	dy											
2	0.1	0.1											
3													
4		psi											
5			1	1	1	1	1	1	1	1	1	1	1
6			0.9										0.9
7			0.8										0.8
8			0.7										0.7
9			0.6										0.6
10			0.5										0.5
11			0.4										0.4
12			0.3				0	0	0				0.3
13			0.2				0	0	0				0.2
14			0.1				0	0	0				0.1
15			0	0	0	0	0	0	0	0	0	0	0

Fig. 1 Spreadsheet for a stream function ψ for flow over a step.